Small Animal PET Imaging with Germanium Strip Detectors

B. F. Phlips, R. A. Kroeger, J. D. Kurfess, W. N. Johnson, *Members, IEEE*

E.A. Wulf, E. I. Novikova

***Abstract*-- We have demonstrated a PET imaging system based on double-sided germanium strip detectors. The demonstration achieved an intrinsic position resolution of 1.35 mm FWHM. This performance was achieved with 2 mm orthogonal strips and a depth sensing capability of 0.5 mm based on timing the pulses at either side of the detector. The system could trigger at energies as low as 15 keV without any image degradation. By selecting events within the 2 keV-wide photopeak, events that scattered within the sampling volume were totally eliminated. If a detector is built with 1 mm strips, the position resolution for PET imaging will not be dominated by the position resolution of the instrument, but by the range of the positron in the sample.**

I. Introduction

Over the last 50 years, Positron Emission Tomography (PET) has evolved from a curiosity into a common clinical and research tool. For the last 30 years, PET designs have mostly been based on rings of scintillating detectors read out by photomultiplier tubes. The evolution and improvements in PET scanners have followed the developments in scintillation materials and photomultiplier tubes. As scintillation materials are developed with better stopping power and faster response times, more sensitive PET systems can be built. With the development of position-sensitive photomultiplier tubes, a new regime of position resolution opened up. Photomultipler tubes are now available with pixels of ~ 2 mm x 2 mm. To optimally use these pixels, newer generation scintillation crystals are segmented into into small pixel arrays. There are now a multitude of PET camera heads [1,2,3] with pixellated Bismuth Germanate (BGO), Gadolinium Orthosilicate (GSO), Lutetium Orthosilicate (LSO), Yttrium Aluminum Perovskite (YAP), etc…

The common feature of these instruments is that there is a very fine two-dimensional square pixellization, typically 2 to 4 mm a side, and an unpixellized third dimension. As the size of the pixels shrinks, the cost in generating these crystals grows, and the fraction of the area taken up by gaps between the crystals grows significantly. The third dimension, the depth, is typically 20 mm. This depth is required to provide sufficient material to stop an annihilation photon with 511 keV of energy. When a gamma ray interacts in a crystal pixel, the location of the interaction is limited to a voxel, or three-dimensional pixel. The size of that voxel is roughly given by the dimensions of the small crystal.

For PET imaging, two such voxels are connected by lines to determine the origin of the radiation. If the radiation is perpendicular to the small face of a crystal, then the depth of the crystal does not contribute to the position uncertainty, and images with a very fine position resolution can be made. This is how on-axis two-dimensional (2D) PET works. Typically, as one moves off axis in a trans-axial plane, the image resolution starts to degrade. This is because the radiation is no longer perpendicular to the small face of the crystal and the long side of the crystal now causes a significant uncertainty in the position. Similarly, if one allows annihilations that are not in a trans-axial plane but have a significant component of their momentum in a sagittal or coronal plane, then the depth of the crystal again starts to contribute to the position uncertainty and the image quality degrades. This is typically the case for three-dimensional (3D) PET.

To overcome the effect of the depth of the crystal, or the depth of interaction (DOI) problem, several approaches can be taken. One is to restrict the imaging to 2D PET. This approach causes a clear loss of efficiency, and thus a similar loss of sensitivity. Another approach is to have a large distance between the ring of the detectors and the sample of interest. If the ring of detectors is large compared to the sample, then the gamma rays originate from near the axis of symmetry, or the center of the ring. The angle of incidence into the crystals is then nearly perpendicular, and the DOI problem decreases. The quantity of detectors required, and therefore the cost, in a

Manuscript received November 20, 2002.

B. F. Phlips, R. A. Kroeger, J. D. Kurfess, and W. N. Johnson are with the Naval Research Laboratory, Washington, DC 20375 USA (telephone: 202-767-3572, e-mail: Phlips @nrl.navy.mil).

E. A. Wulf, is a NRC/NRL Postdoctoral Fellow, Naval Research Laboratory, Washington, DC 20375 USA (telephone: 202-404-1475, e-mail: Wulf @nrl.navy.mil).

E.I. Novikova is with George Mason University, Fairfax VA 22030 USA (telephone: 202-404-1482, e-mail: Novikova@ssd5.nrl.navy.mil).

PET system is proportional to the circumference of the ring. Worse though, is the fact that the solid angle coverage of a certain axial length of detector shrinks as the ring diameter grows. The efficiency then decreases sharply as the ring diameter grows.

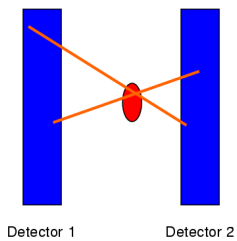

Fig. 1. Schematic diagram of the experimental setup. Detectors 1 and 2 are double-sided germanium strip detectors with 2 mm pitch and 0.5 mm depth resolution. The detectors are 5 x 5 x 1 cm in size and the detector separation was ~9 cm.

New approaches to solving the depth of interaction problem are needed. This is particularly true for PET applications where a large instrument bore and large rings are not necessary, such as small animal PET or Positron Emission Mammography (PEM). Very recently, a number of groups have proposed approaches where some depth of interaction information could be obtained [4,5]. The techniques rely on changing the scintillation properties at different depths in the scintillator. The timing characteristics of the scintillation are altered for different depths. The light pulse collected by the photomultiplier tube from the end of the crystal is then processed with electronics with different time constants to extract the depth information. The scintillation properties are either changed by changing the dopants in the crystals, or by outright change of type of scintillator. The multi-scintillator approach is a pixellated version of the well known phoswich detector concept. The total depth of the crystal can be segmented in 2-4 pieces based on these techniques. These approaches are very laborious, and they can not be extended to much finer depth resolution.

We propose a new approach to PET based not on scintillation detectors but on germanium semi-conducting detectors. Semi-conducting detectors offer multiple advantages over scintillation detectors. The two-dimensional pixellization achieved with mechanical gaps and grooves in scintillators can be achieved by electrical segmentation on a single substrate. This means much smaller gaps can be achieved, and an arbitrarily small pitch can be achieved. Indeed, pixellized silicon detectors with 20-micron pixels are an everyday occurrence in commercial digital cameras. A less well-known feature of semi-conducting detectors is that the depth of interaction can be measured very accurately by timing techniques [6]. The time difference between the appearance of a signal on the top and bottom of a planar semi-conducting detector can be used to derive the depth [7] with great accuracy (< 0.5 mm). This technology is therefore intrinsically capable of excellent three-dimensional localization of gamma ray interactions.

II. Experimental Setup

We have built a prototype PET detection system based on germanium strip detectors [8,9] that have excellent energy resolution and three-dimensional position resolution. A schematic layout of the prototype is shown in figure 1. Two planar germanium detectors were used and the imaged volume is the region between the detectors. Each detector is a germanium double-sided orthogonal strip detector, with an active volume of 5 x 5 x 1 cm. Each surface of the detector has twenty five 2 mm wide strips. By combining the strip information from both sides of the detectors, 2 mm square pixels are generated. The third dimension is obtained by measuring the relative time between the arrival of the collected charge pulse at both electrodes [6]. Wulf et al. [7] showed a position resolution of 0.5 mm could be achieved using the technique in these detectors. The pair of detectors was partially instrumented with electronics reducing the actual sensing area to 8 cm^2 for the first detector, and 10 cm^2 for the second one. The data acquisition system was triggered on coincident events between both detectors with a coincidence window of ~500 ns. Even though the detectors have an excellent energy resolution of ~2 keV, a broad energy window was accepted in order to maximize the efficiency of the system. All events between a lower level discriminator of 15 keV and the 511 keV peak were accepted. All events with valid three-dimensional coordinates in both detectors can be used for image reconstruction.

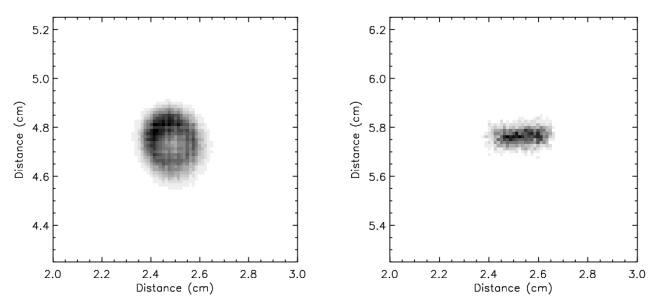

Fig. 2. Reconstructed images of a Na-22 source. Both images are in a reconstructed plane that contains the source and is parallel to the detector planes. The left image has a 1 microCurie source in the plane of the detectors. The right image has the source perpendicular to the detector planes. The right hand picture shows a vertical thickness that corresponds to a position resolution of 1.5 mm Full-Width-at-Half-Maximum.

Since the main goal of this proof of concept was demonstrating the detector performance, only a very simple reconstruction algorithm was used. For each valid event, a line of pixels connecting the two interaction sites was incremented by 1 in the three-dimensional imaged volume. By collecting many events, three-dimensional images can be generated. More sophisticated algorithms can and should be used. Because of the total count limitations of PET, list-mode maximum likelihood reconstructions look the most promising.

Nevertheless, the simple reconstruction algorithm we used does demonstrate the excellent imaging capability of this technology.

III. RESULTS

Figure 2 shows a pair of images of a Na-22 source generated with the setup. The source was a standard calibration source with an unknown source distribution within the sealed capsule. Both images are generated by reconstructing the flux in a plane that both contains the source and is parallel to the detector plane. This plane is found by choosing the slice with the maximum counts per voxel. The left picture of Figure 2 shows that the source distribution is ~ 4 mm in diameter, with a very uneven source distribution. The position resolution is clearly better than the source distribution. The right hand picture of Figure 2 shows the same source rotated by 90 degrees into a roughly horizontal plane. The reconstructed vertical thickness of the source provides an upper limit to the position resolution of the system. Fits at various positions show an upper limit to the resolution of 1.5 mm Full Width at Half Maximum (see Figure 4). This is slightly larger than the resolution expected from the 2 mm pixellization of the detector, although it is also affected by the large third dimension of the source and the spread due to the motion of the positrons as they slow down in the source.

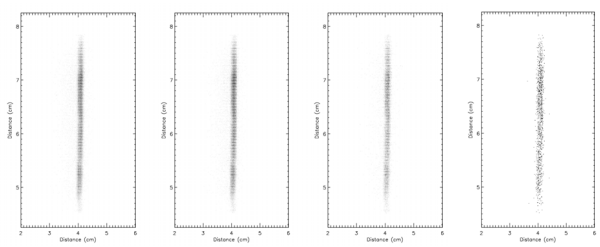

Fig. 3. Reconstructed images of a Ge-68 line source with a 1.5 mm active cross section. The images show the effect of increasing the lower level threshold on the energy of events allowed in for reconstruction. The left most picture has a threshold of 15 keV, followed by thresholds of 50 keV, 200 keV and 500 keV. The right most picture therefore only contains events where both 511 keV gamma rays underwent photoelectric absorption. No image degradation occurs when lowering the threshold, but the efficiency improves dramatically.

Figure 3 shows the reconstructed images from an Isotope Products line source of Germanium –68. The source activity is contained in a cylindrical cavity with a 1.5 mm diameter. The line source is clearly imaged. The four panels illustrate the effect of raising the lower level threshold on the energy deposited in a detector. The image quality is clearly unaffected by the decreasing threshold. The efficiency, on the other hand, is improved as the threshold is lowered. The events are as good as higher energy events in term of reconstructing positions, as clearly proven in Figure 3. Most scintillation-based detectors for PET need to put the threshold substantially higher, leading to a relative loss in efficiency. The right most picture of Figure 3 contains the fewest counts, but all the events are guaranteed to be caused by the photoelectric absorption of 511 keV annihilation photons. This means that the gamma rays are guaranteed to not have interacted anywhere before entering the detector. Any coincidence events caused by scattered radiation are therefore totally eliminated. This mode can be useful when a very high-contrast image is required or when an unusually large amount of scattering material is present.

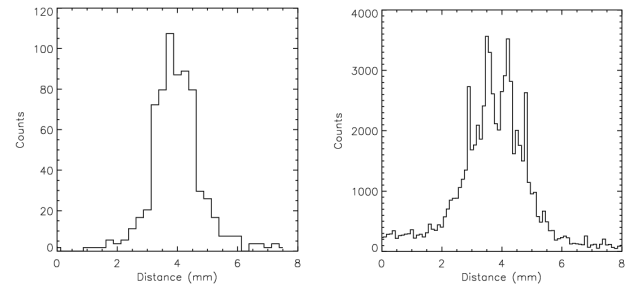

Fig. 4. Left: Vertical cross section through the right hand side image of Figure 2, the image of a side view of a Na-22 source. The Full Width at Half Maximum is 1.5 mm. Right: Horizontal cross section through the left hand picture of Figure 3, the image of a Ge-68 line source. The width is dominated by the size of the source (1.5 mm diameter) and the range of the positrons (~ 1 mm).

The position resolution in the image is measured by studying cross-sections of the images shown in Figures 2 and 3. Figure 4 (Left) shows a vertical cross section through the right side image of Figure 2, the side-view of a Na-22 calibration source. The full-width-at-half-maximum of the distribution is 1.5 mm. Cross sections taken at various other locations gave the same result. Some of this 1.5 mm is due to the distance the positron travels as it slows down before it annihilates. The 540 keV endpoint energy positrons from Na-22 beta-decay have a range of .23 g/cm^2. This corresponds to a 0.85 mm range in any direction in aluminum, or a diameter of 1.7 mm. Since the bulk of the positrons have an energy closer to half the end point, the corresponding range is 0.09 g/cm^2, or a corresponding diameter of 0.7 mm. Subtracting this in quadrature from the measured resolution results in an intrinsic position resolution of 1.3 mm. This corresponds to the expected resolution from the pixellization.

The cross section through the image of the Germanium-68 line source is also shown in Figure 4 (Right). It has a FWHM of 1.9 mm. The source is contained in a steel tube with an outer diameter of 4 mm and an active volume of 1.5 mm diameter. The endpoint energy of the positrons is ~ 1.9 MeV. The range of the positrons in the steel tube is ~ 1 mm. The range of the positrons therefore contributes significantly to the spread of positions from which annihilations can originate. The width shown in Figure 4 is a convolution of three things: the one-dimensional projection of the distribution of source material held in a circular pattern; the range of positrons emanating from the source material; and the position resolution of the imaging system. In order to better understand these issues, we modeled the source in a Monte Carlo simulation program. The GEANT-4 [10] simulation package was used to simulate the materials and particle transport. The package has

been extensively tested and fine-tuned in our laboratory to ensure a good performance for low energy processes [10s of keV to a few MeV]. The cross section of positions where positrons with the endpoint energy of ~1.9 MeV annihilated, when the entire circular source distribution is projected onto one axis, has a FWHM of 2.0 mm. When using a mean positron energy of ~ 1 MeV, the FWHM drops to 1.3 mm. If we subtract this in quadrature from the observed width of 1.9 mm, we again derive an instrument resolution of between 1.3 and 1.4 mm.

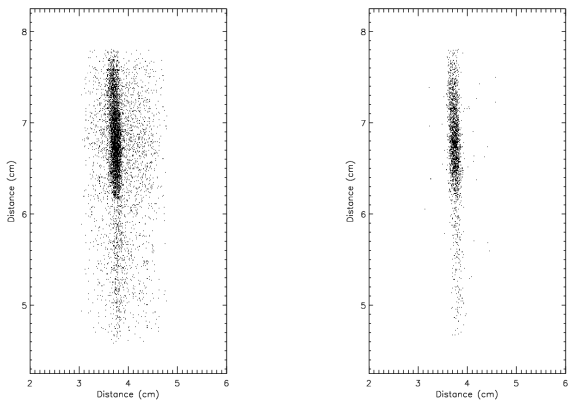

Fig. 5. Reconstructed images of a Ge-68 line source with a 1.5 mm active cross section and a 1 cm thick lead piece covering the bottom half of the field of view. The left hand picture has a threshold of 15 keV, whereas the right hand picture only contains events where both 511 keV gamma rays underwent photoelectric absorption. The photopeak-only image has very few scattered events, even though 1 cm of lead was present.

To demonstrate the rejection capability of the instrument for scattered events, we inserted a 1 cm thick piece of lead in the bottom half of the sensing volume and imaged the line source of Ge-68 (Figure 5). The attenuation due to the lead in clearly visible in the bottom half of the image. The left image shows the reconstructed image with a significant halo due to the events that scattered in the lead. The picture on the right shows the same setup but only includes events that deposited 511 keV in each detector. Almost all scattered events are rejected. This technique reduced the overall efficiency of coincidence detection by a factor of ~ 30 in our laboratory setup. In the proposed instrument, the thicker detectors and improved geometry will reduce this effect to a factor of ~ 8 loss in efficiency. Nevertheless, this mode of operation can be used when sharp contrasts are required and when the increase in radiation dose is not a problem.

IV. Proposed Instrument

We propose a prototype small animal PET system based on double-sided germanium strip detectors. A picture of the proposed instrument is shown in Figure 6. The instrument would consist of four rectangular germanium strip detectors. The detectors would be arranged in a box-type geometry creating an inside volume with a square cross section. The detectors would have an active detector volume of 6.5 x 13 x 1.7 cm and a strip pattern of 64 x 128 strips, or a strip pitch of 1.02 mm. Each strip has its own read-out electronics for spectroscopy and timing. Each detector would be held in an aluminum frame that would also hold printed circuit cards. The four aluminum frames would be held onto a cold frame. The four detectors would be held in a common cryostat and cooled by a common cold plate.

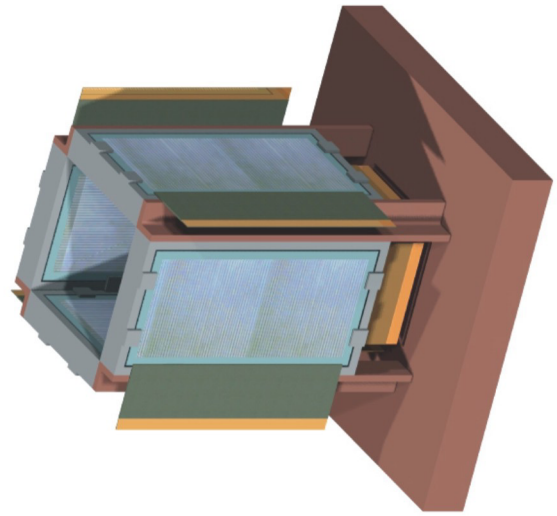

Fig. 6. Artist's impression of the proposed instrument. The instrument consists of 4 germanium strip detectors with a position resolution of 1 mm. Not shown are the cryostat and ribbon cables. The sensing volume of the instrument is 6 cm in diameter, 10 cm long and is in an air environment. The position resolution of the instrument for images in the trans-axial plane will be ~ 0.7 mm FWHM.

Samples would remain in a regular air environment and be inserted in the volume between the detectors. The sensing volume would be a cylinder with a diameter of 6 cm and a depth of 10 cm. The central 4 cm in diameter and 8 centimeters in length would have an absolute coincidence efficiency of >10% (see Figure 7). Based on the 1.3 mm FWHM position resolution obtained in images made with our laboratory proof of concept demonstrator, we expect images in the trans-axial plane to have a position resolution of 0.7 mm FWHM. The position resolution in the third dimension will be somewhat degraded. The readout electronics for the instrument, based on proven commercial VME modules, will be able to operate at >100 kHz. With an average coincidence efficiency of ~10%, this count rate is achieved with a total activity of ~30 microCi, or ~10^6 Bq. A more suitable activity to minimize accidental coincidences would be ~10^5 Bq. A 15 minute exposure could therefore collect ~10 million events. For a 25 gram mouse, if 10% of the volume elements contained all the activity, there would be 4 000 counts per active voxel. The statistical errors would therefore be small (~1.5 %). Figure 8 shows a cutout of the detectors in their cryostat.

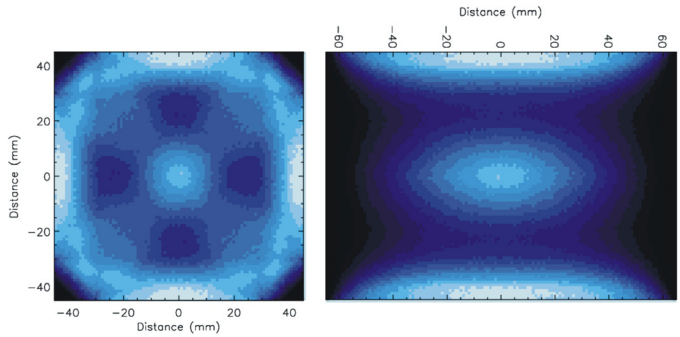

Fig. 7. Coincidence efficiency maps for the proposed instrument. The left hand picture is a trans-axial efficiency map; the right hand view is a sagittal or coronal efficiency map. Because of symmetries, the latter two are equivalent. The brightest regions correspond to 18% efficiency; the darkest regions correspond to 0% efficiency.

V. Conclusions

We have demonstrated Positron Emission Tomography imaging with a position resolution of 1.3-1.4 mm using germanium strip detectors with a 2 mm pitch. If we use detectors with 1 mm strip pitch, an imaging resolution of 0.7 mm should be obtained. At this level one can really start to explore the effect of the different endpoint energies the various possible isotopes. Another factor of two reduction in strip pitch might be possible before one encounters limitations due to the path-length of the conversion electron in the detector material itself.

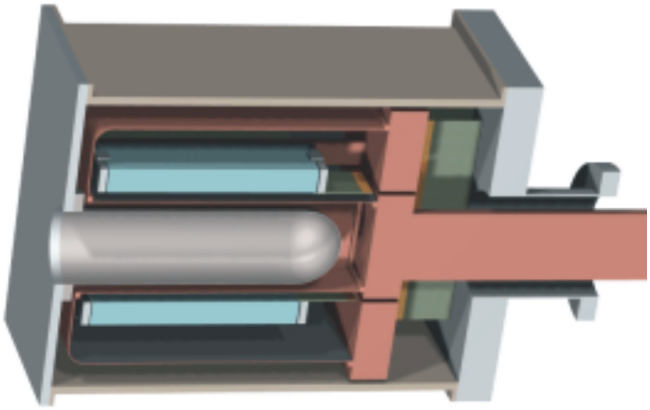

Fig. 8. Cut out view of the proposed cryostat. The cryostat is ~ 30 cm long and 25 cm a wide. The left plate is used to mount the gantry. It can also support a rotation stage to hold and rotate the samples. The cryostat can be mounted horizontally or vertically, but is assumed to be horizontal. Samples are inserted in the central hole.

VI. References

[1] Damiani C, Del Guerra A, Di Domenico G, Gambaccini M, Motta A, Sabba N, Zvattini G, An integrated PET-SPECT imager for small animals. Nucl. Instrum. Methods Phys. Res. Sect. A-Accel. Spectrom. Dect. Assoc. Equip. 2001; 461: 416-419.

[2] Chatziioannou AF, Cherry SR, Shao YP, Silverman RW, Meadors K, Farquhar TH, Pedarsani M, Phelps ME, Performance evaluation of microPET: A high-resolution lutetium oxyorthosilicate PET scanner for animal imaging. J. Nucl. Med. 1999; 40: 1164-1175.

[3] Tzanakos G, Kontaxakis G, Nikolaou M, Panayotakis G, Pavlopoulos S, Skiadas M, Spyrou G, Thireou T, Design and Construction of a Small Animal PET Prototype. IEEE MIC Conf. 2002; M3-181.

[4] Inadama N, Murayama H, Omura T, Yamashita T, Yamamoto S, Ishibashi H, Kawai H, Omi K, Umehara T, Kasahara T, A depth of interaction detector for PET with GSO crystals doped with different amounts of Ce. IEEE Trans. Nucl. Sci. 2002; 49: 629-633.

[5] Kuntner C, Lecoq P, Pizzolotto C, Development of new mixed LuYAP:Ce scintillator crystals for application in a small animal PET scanner with DOI capability. IEEE MIC Conf. 2002; M3-21.

[6] Momayezi M, Warburton WK, and Kroeger R, Position resolution in a ge-strip detector. SPIE 1999; 3768: 530-537.

[7] Wulf EA, Ampe J, Johnson WN, Kroeger RA, Kurfess JD, Phlips BF, Depth Measurement in a Germanium Strip Detector. IEEE Trans. Nucl. Sci. 2002; to be published.

[8] Inderhees SE, Phlips BF, Kroeger RA, Johnson WN, Kinzer RL, Kurfess JD, Graham B, Gehrels N, Spectroscopy, imaging and Compton-scatter polarimetry with a germanium strip detector. IEEE Trans. Nucl. Sci. 1996; 43: 1467-1471.

[9] Phlips BF, Johnson WN, Kroeger RA, Kurfess JD, Phillips G, Wulf EA, Luke PN, Development of germanium strip detectors for environmental remediation. IEEE Trans. Nucl. Sci. 2002; 49: 597-600.

[10] Chauvie S, Ivanchenko V, Longo F, Santin G, Nieminen P, Pia MG, The Geant4 simulation toolkit and its low energy electromagnetic physics package. Med. Phys. 2002; 29: 1231-1231.